ARTICLE

Neutron spectra and dosimetric assessment around a neutron Howitzer container

Sílvia Barros[a*], Eduardo Gallego[b], Alfredo Lorente[b], Isabel F. Gonçalves[a], Pedro Vaz[a], Héctor René Vega-Carrillo[c] and Maria Zankl[d]

[a]IST/CTN, Universidade Técnica de Lisboa, Estrada Nacional 10, ao km 139,7 2695-066 Bobadela LRS, Portugal; [b]Departamento de Ingeniería Nuclear, Universidad Politécnica de Madrid, E-28006, Madrid, España; [c]Unidad Académica de Estudios Nucleares de la Universidad Autónoma de Zacatecas, 98060, Zacatecas, México; [d]Helmholtz Zentrum München German Research Center for Environmental Health, 85764, Neuherberg, Germany

The neutron Howitzer container at the Neutron Measurements Laboratory of the Nuclear Engineering Department of the Polytechnic University of Madrid (UPM), is equipped with a [241]Am-Be neutron source of 74 GBq in its center. The container allows the source to be in either the irradiation or the storage position. To measure the neutron fluence rate spectra around the Howitzer container, measurements were performed using a Bonner spheres spectrometer and the spectra were unfolded using the NSDann program. A calibrated neutron area monitor LB6411 was used to measure the ambient dose equivalent rates, $\dot{H}^*(10)$. Detailed Monte-Carlo simulations were performed to calculate the measured quantities at the same positions. The maximum relative deviation between simulations and measurements was 19.53%. After validation, the simulated model was used to calculate the equivalent dose rate, $\dot{H}_T$, in several key organs of a voxel phantom. The computed $\dot{H}_T$ in the skin and lenses of the eyes are within the ICRP recommended dose limits, as is the $\dot{H}^*(10)$ value for the storage position.

Keywords: neutron dosimetry and spectrometry; BSS; neutron Howitzer; MC simulations; voxel phantom

1. Introduction

The Bonner spheres spectrometer, BSS, has been widely used in neutron dosimetry and spectrometry studies since its introduction by Bramblett, Ewing and Bonner, in 1960 [1]. It is a set of different radii polyethylene spheres in the centers of which thermal neutron detectors are placed. BSS have been used to measure neutron spectra from thermal energies up to 20 MeV and, with some modifications, the neutron energy range may be extended to hundreds of MeV [2]. This is one of the main advantages of this spectrometry technique [3]. On the other hand, major drawbacks are its heavy weight, low energy resolution, the need of a response matrix, the complex unfolding methods and the long period of time needed to irradiate the spheres [3].

The reading, C_i, of the thermal neutron detector inside the ith Bonner sphere when exposed to a neutron field may be expressed by Eq. (1), which is the Fredholm integral, where $R_i(E)$ is the response function of the ith sphere and $\Phi_E(E)$ is the neutron fluence.

$$C_i = \int_{E_{min}}^{E_{max}} R_i(E)\Phi_E(E)dE \qquad (1)$$

Because of the amount of detectors and discrete energy groups, it is necessary to use the discrete version of Eq. (1), expressed by Eq. (2), where N_g is the number of energy groups and m the number of detectors.

$$C_i = \sum_{j=1}^{Ng} R_i(E_j)\,\Phi_E(E_j)\Delta E_j \quad i = 1,2,\dots,m \qquad (2)$$

Because the number of measurements, m, is lower than the number of unknowns, Ng, there is an infinite number of solutions but only a few have physical meaning.

Several unfolding techniques have been developed to obtain the neutron spectrum using the count rates measured with a BSS, such as the least-squares adjustments [4], iteration methods [4] and artificial neural networks (ANN) [5], and numerous unfolding codes use these techniques. Some examples are FRUIT [3] and NSDann [6].

In this work, the NSDann program was used to obtain the neutron energy fluence and $\dot{H}^*(10)$ around a neutron Howitzer container with a 74GBq [241]Am-Be neutron source that can be placed in two positions: irradiation or storage. The Howitzer container exists in the Neutron Measurements Laboratory of the Nuclear Engineering Department of the Polytechnic University of Madrid [8, 9].

To unfold the neutron spectrum, the NSDann

program makes use of artificial neural networks. Because of this, the program user does not need to provide a starting spectrum or any other parameter beyond the count rate of the Bonner spheres, and this is one of the advantages of using NSDann. The unfolded neutron spectrum has associated uncertainties related to the architecture design and learning algorithm and to the experimental uncertainties [4, 7]. The purpose of the present work was to perform the dosimetric assessment and characterization of the neutron field around the Howitzer container for both source positions. To accomplish this objective, measurements using a BSS and a dose-rate meter were performed to determine the neutron spectra and ambient dose equivalent. These quantities were computed performing Monte Carlo (MC) simulations of the experimental setup and the results were compared with measurements. After the model validation, the voxel phantom GOLEM [10] was used to determine the equivalent dose in several key organs, with the source in the irradiation position, to verify that the dose to which a worker is exposed when handling the Howitzer container is within the recommended dose limits presented in ICRP 103 [11] and below the latest dose limits recommended by the ICRP for the lens of the eye (20 mSv/year) [12]. The $\dot{H}^*(10)$ in the phantom's position was also computed for both source positions. Because the ^{241}Am-Be neutron source also generates high-intensive gamma-rays of 4.438 MeV [13], the dose due to neutrons and to gamma-rays was computed separately.

2. Materials and Methods

The Howitzer container has a 57 cm diameter and 86 cm height and is filled with paraffin. It includes an inner axial cylindrical hole to move the neutron source to the central (irradiation) or to the lower (storage) position, by means of a methacrylate bar. When placed in the irradiation position, the source is aligned with two radial cylindrical holes (irradiation tubes). The 74 GBq ^{241}Am-Be neutron source has a cylindrical shape with a 0.740 cm radius and 3.175 cm height, and is covered with a 0.210 cm thick steel cladding.

2.1. Measurements

The Bonner sphere spectrometer used to measure the neutron count rates is composed by a set of six polyethylene spheres (0.95 g.cm^{-3}) with diameters of 0, 5.08, 7.62, 12.7, 20.32, 25.4 and 30.48 cm, where the 0 diameter represents the bare detector. The used thermal neutron detector was a 0.4 cm height and 0.4 cm diameter ^{6}LiI(Eu) scintillator. Count rates were acquired 44.5 cm away from the center of the Howitzer, for both source positions, with the detectors aligned with the source. The acquisition time of each sphere was that appropriate to obtain a statistical uncertainty below 2%. The ambient dose equivalent rate was measured using a dose-rate meter LB6411 [14], at the same position where the count rates were acquired. This instrument was

calibrated with an ^{241}Am-Be source and its H*(10)/ϕ shape is tailored to be in accordance with the recommendations of ICRP 60, from thermal to 20 MeV neutrons [14].Using the measured count rates, the neutron spectra were unfolded using the NSDann program. This unfolding program also determines $\dot{H}^*(10)$.

2.2. Monte Carlo simulations

The detailed geometry and materials of the experimental setup were accurately implemented using the MCNPX 2.7 program [15], in order to calculate the neutron fluence and $\dot{H}^*(10)$. Both ^{6}LiI(Eu) and Bonner spheres were implemented to compute the measured count rates for the two source positions. **Figure 1** shows the MCNPX implemented model of the Howitzer container and a Bonner sphere, for the irradiation and storage source position.
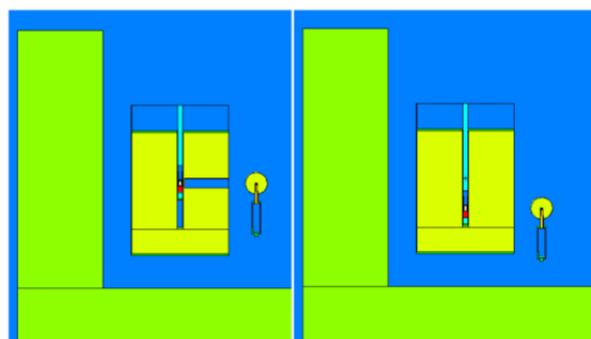

Figure 1. Implemented model of the Howitzer container and a Bonner sphere for the irradiation (left) and storage (right) position.

The used neutron source emission spectrum is the one recommended in ISO 8529 [16, 17]. Following the manufacturer's certificate, the value of the neutron yield of the ^{241}Am-Be source on the day when the measurements were performed, was 4.86×10^6 n.s^{-1}. Since MCNPX does not include the thermal dispersion libraries for paraffin, this material of the Howitzer container was replaced by polyethylene, so the S(α, β) card, or to say, the thermal treatment card, can be included in the simulations. The neutron fluence rate was calculated using a flux averaged over a cell tally (tally F4 in MCNPX terms). Two sets of $\dot{H}^*(10)$ values were then calculated by folding the neutron spectra with both the ICRP74 [18] and the Berthold LB6411 [14] neutron fluence-to-ambient dose equivalent rate conversion coefficients, to evaluate the discrepancies due to the different conversion factors. The voxel phantom GOLEM having average body characteristics was used to compute the dose delivered to several organs. Golem was integrated in the Howitzer container geometry, positioned immediately after the brick structure, as shown in **Figure 2,** which corresponds to a 160 cm distance from the center of the Howitzer. The dose delivered to several organs was computed, both for neutrons and gamma-rays, and the equivalent dose rate,

$\dot{H}_T$, was calculated using the radiation weighting factors from ICRP103 [11].
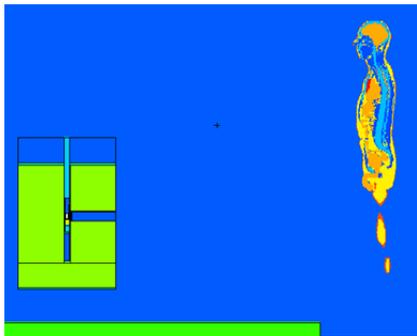

Figure 2. MCNPX implemented Howitzer model and incorporated GOLEM voxel phantom at 160 cm from the center of the Howitzer.

3. Results and Discussion

3.1. Measurements: fluence rate and ambient dose equivalent

The count rates for the irradiation and storage positions that were acquired with the BSS are presented in **Table 1**. These were used in the NSDann unfolding program to obtain the neutron fluence rate spectra, presented in **Figure 3**. **Table 2** displays the total neutron fluence rate and the associated uncertainties which were obtained from the count rates' uncertainties, since the uncertainties related to the unfolding process are not assigned by the unfolding program.

Table 1. Count rates measured with the BSS.

Sphere diameter (cm)	Irradiation position (cps)	Storage position (cps)
Bare	9.58 ± 0.09	1.57 ± 0.01
5.08	12.54 ± 0.12	1.81 ± 0.01
7.62	22.71 ± 0.19	2.53 ± 0.02
12.70	36.88 ± 0.23	3.38 ± 0.02
20.32	27.08 ± 0.22	3.03 ± 0.02
25.40	20.52 ± 0.17	2.37 ± 0.01
30.48	14.10 ± 0.12	1.75 ± 0.01

From Figure 3 it can be observed that the fluence rate significantly decreases when the source is in the storage position, as expected, and both spectra present a maximum for energies around 2-8 MeV, corresponding to the neutrons emitted by the [241]Am-Be source, which are in the energy range from 2 MeV to 8 MeV.

The depression observed in the spectrum for the storage position has no obvious physical reason and is probably due to the NSDann unfolding code limitations stemming from the spectra used to train the artificial neural network.

Table 3 presents both the $\dot{H}^*(10)$ values measured with the calibrated Berthold LB6411 and calculated by NSDann.
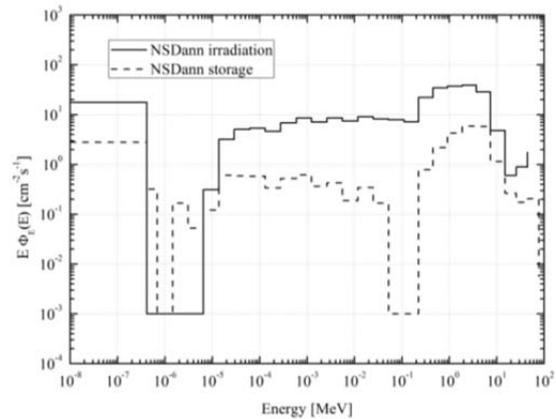

Figure 3. Neutron fluence rate energy spectra with the source in the irradiation and storage positions, obtained with the BSS measurements. The spectra were unfolded with the NSDann unfolding program.

Table 2. Total neutron fluence rate obtained with NSDann.

Total neutron fluence rate (cm^{-2}.s^{-1})	
Source position	NSDann
Irradiation	276.51 ± 2.32
Storage	29.07 ± 0.23

Table 3. Measured ambient dose equivalent rate with the LB6411 and corresponding values obtained using the BSS count rates and NSDann.

$\dot{H}^*(10)$ (µSv/h)			
Source position	LB6411	NSDann	LB6411 vs. NSDann (rel. deviation)
Irradiation	148.93 ± 1.08	164.76	9.61%
Storage	21.72 ± 0.44	20.75	-4.67%

The relative deviation between the measured and calculated values is 9.61% for the irradiation position and 4.67% for the storage position. These deviations may be attributed to the used unfolding technique and also to the different fluence-to-ambient dose equivalent conversion coefficients used by NSDann and by the LB6411 dose-rate meter.

3.2. Monte-Carlo simulations

3.2.1 BSS count rates

In order to compare with measurements, all the Bonner spheres count rates were calculated by means of MC simulations. For this, the ^{6}Li(n,α)^{3}H reactions occurring in the crystal were computed in the MC simulations and multiplied by the crystal's atomic density, active volume and source intensity. This is the way to obtain the count rates of the detection system (Bonner sphere plus ^{6}LiI(Eu) detector).

Table 4 presents, for both source positions, the computed count rates and the deviation to the measured ones. It can be observed that the maximum deviation is 19.53%.

Table 4. Computed count rates and relative deviation to measurements.

sphere diameter (cm)	Irradiation position		Storage position	
	computed count rates (cps)	deviation measured vs. computed	computed count rates (cps)	deviation measured vs. computed
Bare	11.91 ± 0.54	19.53%	1.58 ± 0.08	0.40%
5.08	14.01 ± 0.41	10.51%	2.03 ± 0.06	12.27%
7.62	20.94 ± 0.51	-8.43%	2.54 ± 0.07	0.59%
12.70	33.95 ± 0.65	-8.63%	3.34 ± 0.08	-1.24%
20.32	26.76 ± 0.55	-1.20%	2.90 ± 0.07	-4.44%
25.40	17.31 ± 0.43	-18.53%	2.27 ± 0.06	-4.29%
30.48	12.62 ± 0.36	-11.75%	1.74 ± 0.05	0.42%

3.2.2 Neutron fluence rate

To compare with the unfolded results, the total neutron fluence rate was directly calculated in the simulations, with the same energy bins as used by the NSDann program. In **Table 5** the calculated results are given together with the relative deviations to the values obtained with NSDann. These are 5.25% for the irradiation position and 17.22% for the storage position.

Table 5. MCNPX computed total neutron fluence rate and comparison with the values obtained with NSDann.

Total neutron fluence rate ($cm^{-2}.s^{-1}$)		
Source position	MCNPX	NSDann vs. MCNPX
Irradiation	291.84±0.55	5.25%
Storage	35.12± 0.15	17.22%

3.2.3 Ambient dose equivalent

Both the ICRP74 [18] and Berthold LB6411 [14] H*(10)/ϕ conversion coefficients were folded with the calculated fluence rate spectrum to obtain the $\dot{H}^*(10)$ value. The obtained values, MCNPX$_{ICRP74}$ and MCNPX$_{LB6411}$, respectively, are shown in **Table 6**. The MCNPX $_{LB6411}$ values were those used to compare the simulated values with the measured ones. Compared with the NSDann value, the computed values deviate 1.21% for the irradiation position and 11.73% for the storage position. Compared with the LB6411 values, the deviations of the MCNPX values are 9.29% and 15.65% for the irradiation and storage position, respectively.

Table 6. Computed $\dot{H}^*(10)$, using ICRP74 and LB6411 conversion coefficients, and comparison with measurements.

Source position	$\dot{H}^*(10)$ (µSv/h)			
	MCNPX ICRP74	MCNPX LB6411	MCNPX vs. LB6411	MCNPX vs. NSDann
Irradiation	160.93±0.42	162.76±0.44	9.29%	-1.21%
Storage	18.45±0.12	18.32±0.12	-15.65%	-11.73%

These discrepancies may be attributed to the uncertainties associated with the unfolding methods, but the fact that for the storage position the deviations are higher, may point to the fact that in this situation the simulated neutrons have to travel through the thick wall of the container, thus increasing the influence of the uncertainties associated to the material composition and used libraries.

3.2.4 Voxel phantom: equivalent dose

On the basis of the computed dose rates, annual organ equivalent doses due to neutrons and gamma rays in the selected key organs were estimated for the irradiation position and are shown in **Table 7**. The annual doses were estimated assuming that a worker is exposed to the radiation for 2000 hours per year.

The $\dot{H}^*(10)$ was also computed for the voxel phantom's position, for both neutrons and gamma radiation and both source positions, and these values are presented in **Table 8**.

As can be observed from Table 7, the organs that receive the higher doses are the testes and bladder, because these are the organs that are closest to the beam coming from the Howitzer, and the skin, because it is directly irradiated by the beam. The computed dose in the lenses of the eyes is the dose in both lenses. The computed $\dot{H}_T$ in the skin and lenses of the eyes are lower than the recommended dose limits of ICRP 103. Since the lenses of the eyes are a very small volume and due to computation power issues, the statistical uncertainty of the eye lens dose is around 9%. Despite the relatively high uncertainty, the computed dose value is a good quantitative estimation and it is well below the recommended limit.

Table 7. Annual organ equivalent dose delivered to several organs, with the source in the irradiation position.

Organ	Irradiation position			
	Equivalent dose (mSv/year)			
	Gammas	Neutrons	Total	Limit
Bladder	0.847±0.009	10.267±0.106	11.115±0.106	-
Lenses of the eyes	0.571±0.069	2.613±0.271	3.184±0.280	20
Thyroid	0.581±0.012	3.760±0.109	4.340±0.109	-
Brain	0.381±0.002	1.356±0.021	1.738±0.021	-
Kidneys	0.563±0.003	2.703±0.026	3.266±0.027	-
Testes	1.061±0.020	42.765±0.659	43.826±0.659	-
Skin	0.730±0.001	14.870±0.019	15.600±0.019	500

The recommended effective dose limit for occupational exposure averaged over a period of 5 years is 20 mSv/year which corresponds to approximately 10 µSv/h (for 2000 hours/year). This limit is exceeded when the source is in the irradiation position, but when the source is stored, the value is below the limit, as expected.

Table 8. Computed $\dot{H}^*(10)$ in the voxel phantom's position, using ICRP74 conversion coefficients.

Source position	$\dot{H}^*(10)$ (µSv/h)		
	Gammas	Neutrons	Total
Irradiation	0.633±0.001	18.530±0.105	19.163±0.500
Storage	0.441±0.001	1.213±0.024	1.654±0.852

4. Conclusion

This study shows that Monte Carlo simulations are powerful tools to describe the behavior of detection systems used to perform the spectrometry and dosimetry of neutron radiation fields. The computed results obtained using the implemented model of the setup are consistent with the measurements, taking into account the experimental and computational uncertainties. The maximum relative deviation between measurements and MCNPX computed BSS count rates is 19.53%. Concerning the $\dot{H}^*(10)$ values, the maximum deviation is 15.65% for the storage position. Comparing the $\dot{H}^*(10)$ values obtained with the Berthold LB6411 dose-rate meter and those obtained with the NSDann unfolding program, the differences are, in the worst case, 9.61%. For the irradiation position, the $\dot{H}_T$ in the lenses of the eyes and skin are below the ICRP recommended limits. The computed $\dot{H}^*(10)$ values in the phantom's position exceed 10 μSv/h for the irradiation position. However, the corresponding value when the source is in the storage position is well below this value, showing the efficiency of the Howitzer container to shield the source.

References

[1] R. L. Bramblett, R. I. Ewing and T. W. Bonner, A new type of neutron spectrometer, *Nucl. Instrum. Methods* 9 (1960), pp. 1-12.

[2] R. M. Howell, E. A. Burgett, B. Wiegel and N. E. Hertel, Calibration of a Bonner sphere extension (BSE) for high-energy neutron spectrometry, *Radiat. Meas.* 45 (2010), pp. 1233-1237.

[3] R. Bedogni, C. Domingo, A. Esposito and F. Fernández, FRUIT: an operational tool for multisphere spectrometry in workplaces, *Nucl. Instrum. Methods Phys. Res.* A 580 (2007), pp. 1301–1309.

[4] M. Matzke, Propagation of uncertainties in unfolding procedures, *Nucl. Instrum. Methods Phys. Res.* A 476 (2002), pp. 230-241.

[5] H. R. Vega-Carrillo, V. M. Hernández-Dávila, E. Manzanares-Acuña, G. A. Mercado, E. Gallego, A. Lorente, W. A. Perales-Muñoz and J. A. Robles-Rodrígues, Artificial neural networks in neutron dosimetry, *Radiat. Prot. Dosim.* 118 (2006), pp. 251-259.

[6] M. R. Martinez-Blanco, J. M. Ortiz-Roriguez and H. R. Vega-Carrillo, NSDann, a LabVIEW tool for neutron spectrometry and dosimetry based on the RDANN methodology, *Electronics, Robotics and Automotive Mechanics Conference, CERMA ´09,* (2009).

[7] R. Bedogni, Neutron spectrometry using Bonner spheres, *CONRAD WP4 workshop on "Uncertainty Assessment in Computational Dosimetry: A Comparison of Approaches",* (2007).

[8] E. Gallego, A. Lorente and H. R Vega-Carrillo, Characteristics of the neutron field of the facility at DIN-UPM, *Radiat. Prot. Dosim.* 110 (2004), pp. 73-79.

[9] S. Barros, E. Gallego, A. Lorente, I. Gonçalves, P. Vaz and H. R Vega-Carrillo, Dosimetric assessment and characterization of the neutron field around a Howitzer container using a Bonner Sphere Spectrometer, Monte Carlo simulations and the NSDann and NSDUAZ unfolding codes, *Radiat. Prot. Dosim.,* accepted for publication, *(2012).*

[10] M. Zankl and A. Wittmann, The adult male voxel model 'Golem' segmented from whole body CT patient data, *Radiat. Environ. Biophys.* 40 (2001), pp. 153–622.

[11] ICRP, The 2007 Recommendations of the International Commission on Radiological Protection, ICRP Publication 103, *Ann. ICRP* 37.

[12] ICRP, ICRP Statement on Tissue Reactions and Early and Late Effects of Radiation in Normal Tissues and Organs – Threshold Doses for Tissue Reactions in a Radiation Protection Context, ICRP Publication 118, Ann. ICRP 42.

[13] H. M. Hakimabad, R. Izadi, A. R. Vejdani and H. Panjeh, Reduction of the gamma dose equivalent due to ^{252}Cf and ^{241}Am-Be neutron sources in the patients soft tissues when using body chemical composition analyzer bed, *Asian J. Exp. Sci.* 21 (2007), pp. 133-144.

[14] B. Burgkhardt, G. Fieg, A. Klett, A. Plewnia and B. R. L. Siebert, The neutron fluence and H*(10) response of the New LB6411 Rem Counter, *Radiat. Prot. Dosim.* 70 (1997), pp. 361-364.

[15] D. B. Pelowitz, *MCNPX 2.7. A Extensions*, LANL Report LA-UR-08-07182, Los Alamos, (2008).

[16] International Organization for Standardization, Reference Neutron Radiations, Characteristics and Methods of Production, ISO-Standard 8529, Part 1 (2001).

[17] International Organization for Standardization, Reference Neutron Radiations, Calibration Fundamentals of Radiation Protection Devices Related to the Basic Quantities Characterizing the Radiation Field, ISO-Standard 8529, Part 2, (2000).

[18] ICRP Conversion Coefficients for use in Radiological Protection against External Radiation, ICRP Publication 74, *Annals of the ICRP* 26 (1996).